

Simulation of Solid Particle Passage in Constrained Microfluidic Channel

M.A. Cartas-Ayala*¹, R. Karnik¹

¹Massachusetts Institute of Technology

*Corresponding author:

Room 3-461, 77 Massachusetts Ave., Cambridge Ma., U.S.A., 02139.

mcartas@mit.edu

Abstract: Characterization of deformable particles, e.g. cells, has numerous applications in science and diagnostics. Recently, particle passage through constrained square microchannels has been proposed to characterize particles based on their passage velocity. Nevertheless, there is no clear understanding of how the physics in this system interact. Recently we proposed a model that takes into consideration the gap between the walls and the particle and that regulates the pressure drop that pushes the particle through the microchannel. Here we quantify the effects of the gap flow by simulating the passage of a solid deformed particle moving at different velocities in a microfluidic channel. The fundamental understanding gained through this work could explain differences on the experimental results already available on particle passage through micro channels and filters.

Keywords: Deformability, cells, friction force, passage time, velocity.

1. Introduction

The behavior of particles in flows has been long used to characterize and sort particles suspended in fluids, e.g. centrifugation is routinely used to separate biological samples of multiple constituents. Recently, the ability to build microchannels, a byproduct of the miniaturization techniques used in electronics, has led to the creation of highly controllable environments to characterize particles. These new microenvironments have been used to characterize droplets, microspheres and cells¹.

One of the most studied particles in microfluidic environments are cells. Recently, cell passage through constrained microfluidic environments has been proposed as a tool for characterization of cells. Cell passage time and cell velocity has been used as an indirect tool for measuring cell mechanics, which is an important biophysical

property since cell stiffness can be related to disease states such as cancer and malaria². It has been observed that the rigidity of cells increase the cells transit time; the stiffer the cell the slower it will travel through a microfluidic channel. Nevertheless it is unclear how is that stiffness is related to the other cell passage variables, how the physics involved are related and to what extent and proportion they affect the cell transit variables. Further even the role of the cell's deformed geometry is unclear.

Here we will examine the flow forces that arise exclusively from a deformed particle traveling through a microchannel at a velocity different than the average flow velocity. The present investigation has the objective to highlight and isolate the contributions and effects of the fluid surrounding the particle, which can be used to clarify the nature of the particle-channel interactions in the case of cells.

2. Governing Equations

The equation used during the simulation of the deformed particle traveling through a microfluidic channel are the full Navier-Stokes equations

$$\begin{aligned} \rho \frac{\partial \vec{u}}{\partial t} - \nabla \cdot \eta (\nabla \vec{u} + (\nabla \vec{u})^T) + \\ \rho (\vec{u} \cdot \nabla) \vec{u} + \nabla p = \vec{F}, \\ \nabla \cdot \vec{u} = 0, \end{aligned}$$

where ρ is the fluid density, \vec{u} is the velocity vector field, η is the fluid viscosity, p is the scalar pressure field, and \vec{F} is the volume force vector field.

Here, we kept the inertia terms to check if they have any significant contribution at Reynolds numbers of the order ~ 0.2 .

Finally, we prescribed the velocities at all the boundaries as described in the geometry section.

3. Numerical Model

In order to simulate the particle passage we created a channel geometry of $6 \mu\text{m}$ -square cross-section and $50 \mu\text{m}$ length. At the middle of the channel we subtracted a pill-shape volume, which represents the deformed particle. The pill has rounded front and back ends and leaves a gap between the pill and the channel's corners. Also the pill intersects, i.e. touches, the channel walls, hence preventing flow passage at the channel walls but not the corners.

Two types of corner gaps between the particle and the channel were explored: triangular and rounded. In both models the channel width, H , and the back and front particle radius, $R_2 = 2 \mu\text{m}$, were kept constant.

In the rounded gap model, the gap external radius, $R_1 = 0.5 \mu\text{m}$, and particle length, L_p , were kept constant. In the simulations, the cell velocity (particle velocity) and the fluid flow (inlet velocity) are imposed through boundary conditions (**Fig. 1**). In terms of boundary conditions, a uniform velocity was applied to the inlet and at the outlet the pressure was set to zero. The effects of the particle moving at a non-zero velocity, $u_{particle}$, were implemented by changing the boundary conditions at all the remaining channel boundaries while keeping the velocities at the particle surfaces equal to zero, i.e.

$$u_{wall} = -u_{particle},$$

and

$$u_{particle_wall} = 0,$$

which implies that the inlet velocity is

$$u_{inlet} = u_{fluid} - u_{particle}.$$

In the triangular gap model, the gap side, R_1 , and particle length, l , were modulated. For this model we use an isosceles triangular corner geometry whose dimensions were varied from 0.5 to 2.5

μm (**Fig. 2**). Further, we varied the particles length from 7 to $20 \mu\text{m}$. In this case, the particle velocity was set to zero, i.e.

$$u_{wall} = 0,$$

and

$$u_{particle_wall} = 0,$$

which implies that the inlet velocity is

$$u_{inlet} = u_{fluid}.$$

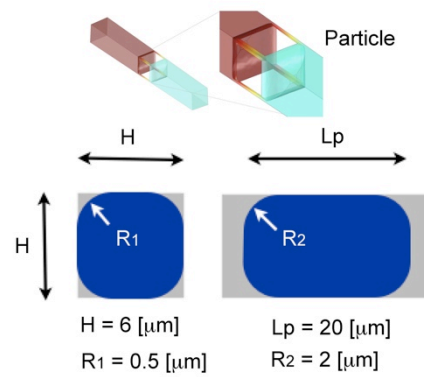


Figure 1. Particle model with round gap.

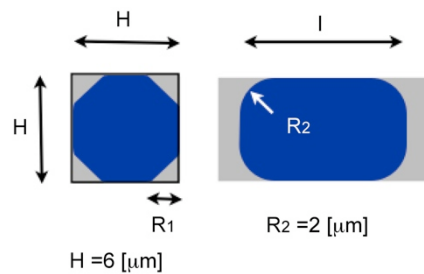


Figure 2. Particle model geometry with triangular corners.

4. Results and Discussion

A representative plot of the pressure distribution is shown in **Fig. 3**. From the plot we can observe that, upstream and downstream the particle, the pressure is roughly uniform. Further, the pressure drop is roughly linear through the gaps between the particle and the channel. Therefore the

pressure drop due to the particle presence is, to any practical purpose, not affected by the particle's back and front geometry. At the gap, the cross sectional channel area becomes less than 1% the area of the open channel, therefore the hydraulic resistance of this section is much larger than that of the unoccupied channel. More precisely, since the viscous hydraulic resistance scales as $\sim 1/a^4$, where a is the characteristic channel size, the resistance per unit length of the gap is 1000 times larger than the resistance per unit length of the channel. Therefore the geometry elsewhere is unimportant.

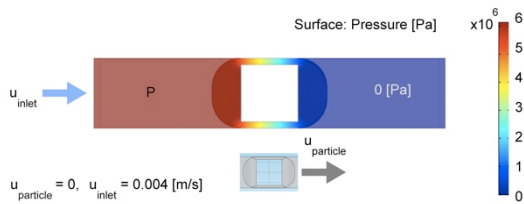


Figure 3. Representative pressure field distribution and boundary conditions applied to a static particle inside a square channel.

Round Gap Model

We found that for this model, for Reynolds numbers up to 0.2, the pressure difference between the particle's back and front scales linearly with the inlet velocity (**Fig. 3**), therefore the effects of inertia are not significant, even when the Reynolds numbers are not much more smaller than one. Hence, viscous dissipation should suffice to describe the forces involved during particle passage.

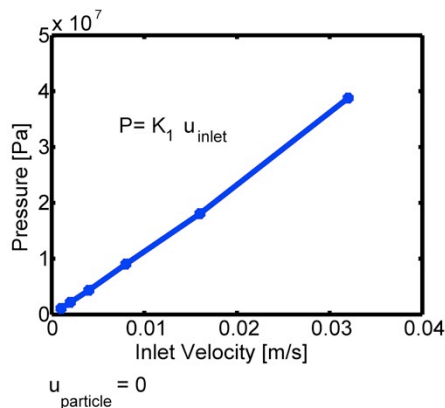


Figure 3. Pressure difference between the back and front ends of the particle with round gaps (static particle) as a function of the inlet velocity.

Additionally, the pressure difference between the cell's back and front decreases approximately linearly with the particle's velocity till the particle's velocity becomes approximately equal to the average inlet velocity (**Fig. 4**). Hence,

$$P = K_1 * u_{inlet} \left(1 - \frac{u_{particle}}{u_{inlet}} \right),$$

where P is the pressure difference between the back and the front of the particle.

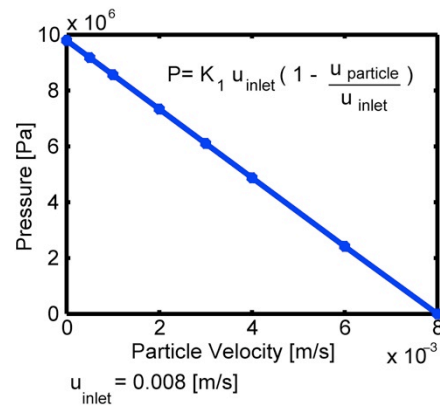


Figure 4. Pressure difference between the back and front ends of the particle with round gaps (static particle) as a function of particle velocity.

Triangular Gap Model

Finally, we studied the effects of the variation of the particle's dimensions. First we explore the effects of the particle's length (**Fig.5**). As expected from a viscous dissipation model, the pressure drop increased linearly with particle length. Nevertheless, there is a small offset of the length-pressure curve; the pressure only starts to grow after an initial length, $\sim 1.5 \mu\text{m}$. A fraction of the total length does not induce a significant pressure drop since that length is lost into creating the back and front parts of the particle, which induce small resistances when compared to the gap section.

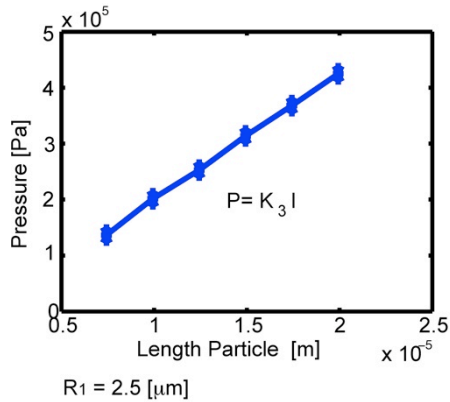


Figure 5. Pressure difference between the back and front ends of the particle with triangular gaps (static particle) as a function of particle length.

Further, we studied the effects of the corner gap size between the particle and the channel walls (**Fig. 6 and Fig. 7**). The pressure difference between the particle's back and front decreased as the gap size increased. The pressure dropped as $\sim 1/R^n$, where R is the length of one of the sides of the triangle and n is a number between 3.5-4; which agrees with the expected behavior of a highly viscous hydrodynamic resistance.

5. Conclusions

In this paper we developed a numerical model that describes the basic forces induced by a large deformable particle flowing through a microfluidic channel. We found that, at least, up to Reynolds ~ 0.2 , the system can be described as a highly viscous problem without significant departures caused by inertia. Further, the pressure drop across the particle is caused by the gap between the particle and the channel without significant contribution from the front and back ends of the particle. Hence the induced pressure drop is directly proportional to the particles length and inversely proportional to the gap size.

Finally, the pressure drop across the particle can be calculated as

$$P = K_2 \left(\frac{l}{R_1^n} \right) * u_{inlet} \left(1 - \frac{u_{particle}}{u_{inlet}} \right),$$

where K_2 is a function of the fluid viscosity and exact gap geometry.

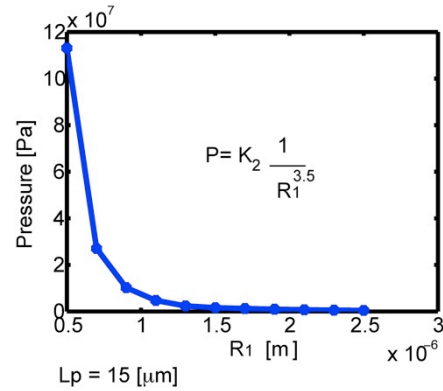


Figure 6. Pressure difference between the back and front ends of the particle with triangular gaps (static particle) as a function of gap size.

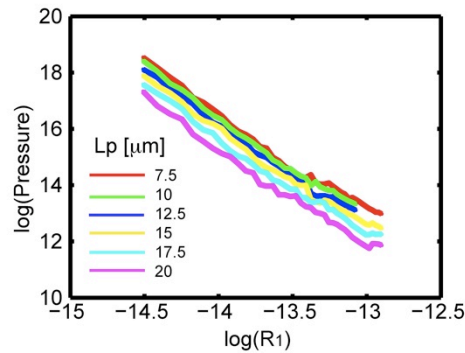


Figure 7. Pressure difference between the back and front ends of the particle with triangular gaps (static particle) as a function of gap size and particle length.

6. References

1. Tan Y, et al., Design of microfluidic channel geometries for the control of droplet volume, chemical concentration and sorting, *Lab Chip*, **4**, 292-298 (2004).
2. Cranston H A, et al., Plasmodium falciparum maturation abolishes physiologic red cell deformability, *Science*, **223**, 400-403 (1984).

9. Acknowledgements

We acknowledge financial support from the Mexican National Science Foundation, CONACYT grant 205899.